

Solvent Effect on the Excited-State Dynamics of Analogues of the Photoactive Yellow Protein Chromophore

Agathe Espagne, Pascale Changenet-Barret,* Pascal Plaza, and Monique M. Martin

Département de Chimie, Ecole Normale Supérieure (UMR CNRS 8640 PASTEUR), 24 rue Lhomond, 75231 Paris Cedex 05, France

Received: November 4, 2005; In Final Form: December 24, 2005

We previously reported that two analogues of the Photoactive Yellow Protein chromophore, *trans-p*-hydroxycinnamic acid (pCA^{2-}) and its amide derivative (pCM^-) in their deprotonated forms, undergo a *trans*–*cis* photoisomerization whereas the thioester derivative, *trans-p*-hydroxythiophenyl cinnamate (pCT^-), does not. pCT^- is also the only one to exhibit a short-lived intermediate on its excited-state deactivation pathway. We here further stress the existence of two different relaxation mechanisms for these molecules and examine the reaction coordinates involved. We looked at the effect of the solvent properties (viscosity, polarity, solvation dynamics) on their excited-state relaxation dynamics, probed by ultrafast transient absorption spectroscopy. Sensitivity to the solvent properties is found to be larger for pCT^- than for pCA^{2-} and pCM^- . This difference is considered to reveal that either the relaxation pathway or the reaction coordinate is different for these two classes of analogues. It is also found to be correlated to the electron donor–acceptor character of the molecule. We attribute the excited-state deactivation of analogues bearing a weaker acceptor group, pCA^{2-} and pCM^- , to a stilbene-like photoisomerization mechanism with the concerted rotation of the ethylenic bond and one adjacent single bond. For pCT^- , which contains a stronger acceptor group, we consider a photoisomerization mechanism mainly involving the single torsion of the ethylenic bond. The excited-state deactivation of pCT^- would lead to the formation of a ground-state intermediate at the “perp” geometry, which would return to the initial *trans* conformation without net isomerization.

1. Introduction

Understanding the structure–function relationship of matter at the atomic scale is a major challenge for chemistry. In this field biology certainly is a source of inspiration. Of particular interest in this context is the ability of some microorganisms to modulate or modify their motile behavior as a function of the illumination conditions of their environment.¹ At the cellular scale, the movement is produced by a motor apparatus, often made of flagellae or ciliae. At the molecular scale, it is initiated within a photoreceptor made of a chromophore bound to a protein. In addition to its fundamental interest, understanding how such natural photoreceptors work is a prerequisite to future advances in biotechnologies. It opens up interesting perspectives for the development of new nanodevices mimicking the capabilities of biological systems to convert light into a signal, ultimately leading to mechanical, chemical or electrical energy release.

One of the better known photoreceptor proteins involved in the photomovement of microorganisms is the Photoactive Yellow Protein (PYP). It was first isolated from the cytosol of the bacterium *Halorhodospira halophila*² and is thought to initiate its behavioral avoidance response to blue light.³ PYP contains a 4-hydroxycinnamoyl chromophore covalently linked to the side chain of its unique cysteine residue (Cys69) by a thioester bond.^{4,5} The chromophore is embedded in the main hydrophobic core of PYP, which isolates it from the solvent.^{6,7} In the ground state, it is deprotonated⁸ and in the *trans*

configuration.^{4,5} Upon irradiation with blue light, PYP undergoes a photocycle involving both chromophore and protein structural relaxations^{9–13} and characterized by several spectroscopic intermediates formed on time scales spanning from several hundred femtoseconds to seconds.^{14–29} *Trans* to *cis* photoisomerization of the chromophore was clearly identified as the first overall molecular process of the photocycle,³⁰ the formation of a relaxed *cis* isomer (I_1) occurring in a few nanoseconds.^{9,13} The internal and external coordinates involved in the photoisomerization reaction path on the femtosecond and picosecond time scale are nevertheless still debated.^{23,24,28,31–38}

The intrinsic photophysics of the isolated PYP chromophore in solution has attracted a growing interest over the past few years.^{27,29,39–47} As a matter of fact, its detailed understanding is a crucial prerequisite to shed light on the isomerization mechanism of PYP. One of the key questions motivating this effort is to know whether the short-time dynamics of PYP is controlled by the intrinsic properties of the chromophore or by the protein environment. In addition, the chromophore is a prime model system for the protein, on which minimal requirements to achieve function can easily be tested by varying substituents as well as the environment.

We already reported the subpicosecond transient-absorption study of three deprotonated analogues of the PYP chromophore in aqueous solution: *trans-p*-hydroxycinnamate (pCA^{2-}), *trans-p*-hydroxycinnamide (pCM^-) and *trans-p*-hydroxythiophenyl cinnamate (pCT^-).^{27,29,39,40,45} These first results emphasized a major effect of chemical structure on the excited-state relaxation dynamics of the molecules. The decay of the excited-state bands of pCA^{2-} and pCM^- , in 10 and 4 ps respectively,

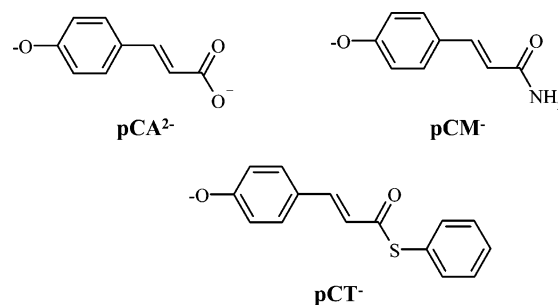
* Corresponding author. Tel: +33 144 322 413. Fax: +33 144 323 325. E-mail: pascale.changenet@ens.fr.

without any detectable intermediate,^{27,29,39,45} was correlated to the net trans to cis isomerization reaction, which was shown to occur by steady-state photolysis associated to ¹H NMR spectroscopy.^{27,45} Single-wavelength probe experiment carried out in the spectral region where the cis isomer absorption dominates indeed highlighted the concomitant rise of a small long-lived absorption band, attributed to the ground-state cis isomer.³⁹ The proposed mechanism was comparable to that of *trans*-stilbene in solution:⁴⁸ the trans excited state decays through a small barrier to a nonpopulated intermediate structure (“perp” state) that leads to both the ground-state cis and trans isomers. On the contrary, the early stage of the excited-state deactivation of deprotonated *trans*-*S*-thiophenyl-*p*-hydroxycinnamate was found to involve, in less than 2 ps, the formation of a detectable intermediate, spectroscopically similar to the first intermediate of PYP (*I*₀^{17,19,23,25–27,29}). The formation of the ground-state cis isomer has never been proved in this case.^{27,29,40,45} Different *p*-hydroxycinnamic acid derivatives with various chemical structures have been studied by other groups, using experimental methods such as pump–dump–probe spectroscopy,^{42,47} fluorescence up-conversion,⁴⁴ Stark spectroscopy⁴³ and visible–pump–infrared–probe spectroscopy,⁴⁶ besides UV–visible transient absorption spectroscopy.^{41,47} These studies revealed a profound effect of the protonation state of the phenol ring, as well as its substitution with electron acceptor groups, on the excited-state lifetime of *trans*-*p*-hydroxycinnamic acid derivatives,⁴⁷ suggesting that charge transfer is a plausible reaction coordinate for the excited-state deactivation. In parallel to this experimental work, quantum chemical calculations and theoretical studies have been performed on *trans*-*p*-hydroxycinnamic acid derivatives.^{49–55} Simulations carried out on a thioester derivative in vacuo predicted that the evolution on the excited-state potential energy surface after excitation involves the torsion of the single bond adjacent to the double bond on the phenolate side rather than that of the double bond, leading back to the original configuration without a significant conformational change.⁵⁴

Despite experimental and theoretical efforts, the nature of the reaction coordinates involved in the excited-state relaxation of *trans*-*p*-hydroxycinnamic acid derivatives remains thus to be clarified. Several isomerization mechanisms could be considered and intramolecular charge transfer could be either involved in it or compete with it. The cis–trans photoisomerization of stilbene requires a large-amplitude relative rotation of the two phenyl substituents, experiencing solvent hydrodynamic friction,⁴⁸ thus viscosity effects. On the contrary, the “hula-twist” isomerization mechanism postulated for polyenes, which proceeds along a volume-conserving coordinate, may not be very sensitive to solvent friction.⁵⁶ Charge reorganization processes are expected to be influenced by polarity and solvation dynamics. Solvent effects on the dynamics may thus give information about the coordinates involved in the excited-state relaxation of *trans*-*p*-hydroxycinnamic acid derivatives. However, no such study has been reported until now.

In this paper, we investigate the effect of the solvent on the excited-state relaxation dynamics of the three deprotonated *trans*-*p*-hydroxycinnamic acid derivatives sketched in Chart 1. The effects of viscosity, polarity, solvation dynamics and solvent hydrogen-bonding donor character are analyzed. The general objective of this study is to stress further the existence of two different relaxation pathways in these compounds and to examine various hypotheses on the coordinates involved. The ultrafast photoinduced events were probed by means of sub-picosecond UV–visible transient absorption spectroscopy.

CHART 1: Molecular Structures of Deprotonated *trans*-*p*-Hydroxycinnamic Acid (pCA²⁻) and Its Amide (pCM⁻) and Thioester (pCT⁻) Analogues



2. Materials and Methods

2.1. Materials. *Trans*-*p*-hydroxycinnamic acid (pCAH₂) was purchased from Sigma-Aldrich. *Trans*-*p*-hydroxycinnamide (pCMH) and *trans*-*p*-hydroxythiophenyl cinnamate (pCTH) were synthesized following procedures described elsewhere.⁴⁰ Samples of pCA²⁻ and pCM⁻ were prepared in water and a series of linear alcohols and ethylene glycol with 0.05 M KOH to achieve complete deprotonation. Samples of pCT⁻ were prepared in a borate Britton–Robinson buffer at pH 10.2 and in alcohols with 5 × 10⁻⁴ M KOH to achieve 95% deprotonation and to avoid hydrolysis during the experiments. The optical density of the samples was adjusted to 1 per mm for steady-state absorption and transient absorption measurements and to 0.1 per cm for steady-state fluorescence measurements. The different solvents used were HPLC grade water and Merck Uvasol methanol, ethanol and 1-butanol. Ethylene glycol and dimethylformamide (DMF) were UV spectroscopy grade solvents (Fluka). 98%-pure 1-propanol, 1-pentanol, and 1-octanol were purchased from Merck and 99%-pure decanol-1 from Acros Organics.

2.2. Steady-State Spectroscopy. Steady-state spectra were recorded with a double-beam UV–visible spectrometer (SAFAS UVmc2) and a spectrofluorometer (Jobin Yvon Horiba Fluoromax 3). Fluorescence spectra were corrected from the instrumental wavelength-dependent response. To get information on the electronic transitions involved in the absorption spectra of the three *trans*-*p*-hydroxycinnamic acid derivatives, steady-state fluorescence polarization measurements were carried out in ethylene glycol. In this viscous solvent, rotational diffusion was found to be negligible during the excited-state lifetime. The anisotropy is defined by

$$r = (I_{\parallel} - I_{\perp}) / (I_{\parallel} + 2I_{\perp})$$

with *I*_∥ and *I*_⊥ the corrected fluorescence intensities with polarization respectively parallel and perpendicular to that of the excitation beam.⁵⁷ The anisotropy was measured by detecting the fluorescence intensity at its peak maximum and by scanning the excitation wavelength over the whole spectral range corresponding to the absorption spectrum.

2.3. Transient Spectroscopy. Transient absorption measurements were performed by the pump–probe technique using a homemade dye laser described in detail elsewhere.⁵⁸ For the present study, 500 fs pulses were generated simultaneously at 355 nm (or 430 nm) and 570 nm. Typically, 50–100 μJ of the 355 nm (or 430 nm) were focused to a diameter of 2 mm in the sample cell and used as the pump. The probe was a white-light continuum generated in a 1 cm water cell from the pulses at 570 nm. Pump and probe polarizations were set at the magic angle. The differential absorbance spectra ($\Delta A(\lambda, t) = A(\lambda, t) -$

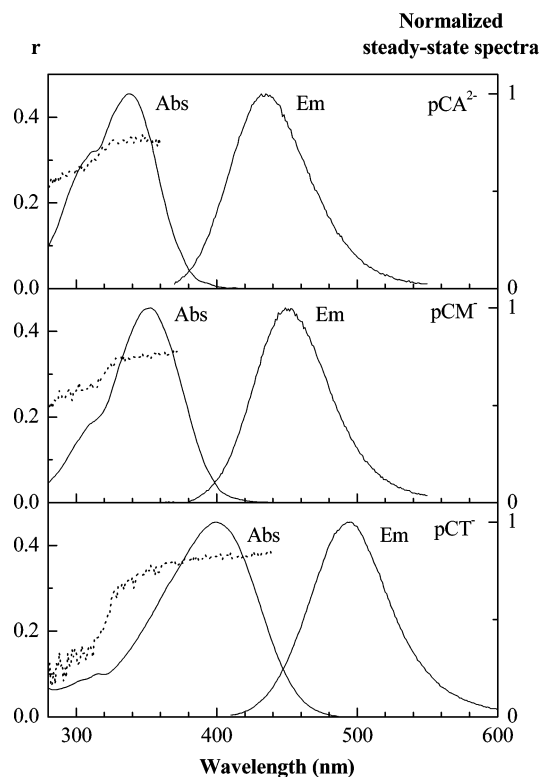


Figure 1. Normalized steady-state absorption and fluorescence spectra of pCA^{2-} , pCM^- , and pCT^- in ethylene glycol. The anisotropy parameter associated with each analogue is shown in dotted line.

$A_0(\lambda)$, where $A(\lambda, t)$ is the excited sample absorbance and $A_0(\lambda)$ the steady-state absorbance) were recorded in the 340–700 nm spectral range, through a spectrograph (Jobin Yvon Spex 270M, entrance slit 64 μm), by a CCD camera (Roper Scientific, 1024 \times 128). The sample solution was recirculated at room temperature through a 1 mm cell. The differential spectra were averaged over 500 laser shots and corrected from group velocity dispersion in the probe beam. Kinetics at selected wavelengths ($\Delta A(t)$) were fitted to a sum of exponentials convoluted by a Gaussian function representing the experimental resolution, the fwhm of which was adjusted to about 1.5 ps.

The steady-state absorption spectrum of each sample was measured before and after each pump–probe experiment, to check for any sample degradation during the experiment. pCT^- samples were found to be chemically unstable during the pump–probe experiments due to solvolysis (hydrolysis in water²⁷). The reaction induces a loss in the sample optical density at the excitation wavelength, and a loss in the intensity of the time-resolved spectra. Because, at the excitation wavelength (430 nm), the reaction product does not absorb, the shape of the time-resolved differential absorbance spectra remains rigorously unaltered by this reaction. The linear correlation between the loss of intensity of the time-resolved spectra and that of the steady-state spectra allowed a straightforward correction.

3. Results

3.1. Steady-State Spectroscopy. Absorption, Fluorescence and Anisotropy Measurements. The absorption and fluorescence spectra of deprotonated *trans-p*-hydroxycinnamic acid and its two analogues in ethylene glycol are displayed in Figure 1. The absorption maxima of pCA^{2-} and pCM^- are located at 340 and 350 nm, respectively, and the spectra exhibit a distinct shoulder on their blue side around 310 nm. The absorption spectrum of pCT^- is 60 nm red-shifted compared to that of pCA^{2-} . The

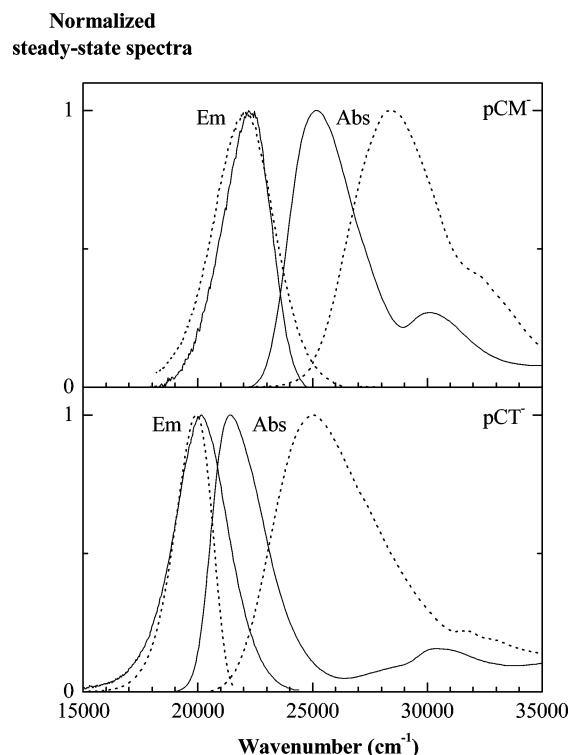


Figure 2. Normalized steady-state absorption and fluorescence spectra of pCM^- and pCT^- in DMF with 1% water and 0.5 M NaOH (plain line) and in ethylene glycol (dotted line).

three compounds are weakly fluorescent. Their quantum yields of fluorescence are estimated to be lower than 1% in water.^{29,39,40} The fluorescence spectra of pCA^{2-} , pCM^- , and pCT^- are centered around 435, 450, and 495 nm, respectively.

The fluorescence anisotropy excitation spectrum of the three compounds is given, in dotted line, in Figure 1. For pCA^{2-} and pCM^- , the anisotropy is found to be a constant of about 0.35 over the 320–370 nm range, corresponding to the main absorption peak. In the spectral region below 320 nm, corresponding to the shoulder, the anisotropy drops down to 0.25. This change indicates clearly the presence of two electronic transitions with different polarization directions.

The anisotropy measured for pCT^- is found to be about 0.37 over the spectral region of the main absorption band, and to drop drastically to 0.13 in the spectral region below 325 nm, corresponding to the electronic transition located around 310 nm. The possible existence of two electronic transitions lying under the main absorption band of pCT^- has already been proposed to explain why it is broader than the emission spectrum.^{27,29,40} The slight decay of the anisotropy observed on the blue side of the main absorption band of pCT^- may indeed reveal the presence of a nearby transition, although it may just come from the upper electronic transition at 310 nm partially overlapping the main absorption band. From Figure 1, one can think that this 310 nm transition corresponds to the shoulder on the absorption spectra of pCA^{2-} and pCM^- . This band has been attributed to the $n \rightarrow \pi^*$ transition located on the carbonyl group of the chromophore.⁵⁹

Steady-State Spectroscopy in Protic and Nonprotic Solvents. The absorption and fluorescence spectra of pCM^- and pCT^- measured in DMF, containing 1% water and 0.5 M NaOH, are shown in Figure 2. For comparison, the spectra in ethylene glycol are also given in dotted line. It is seen that the main absorption band of both pCM^- and pCT^- in DMF exhibits a red shift of about 3300 cm^{-1} with respect to that measured in

ethylene glycol. Interestingly, the upper electronic transition (shoulder around 310 nm) does not exhibit such a shift, which explains why the two absorption bands of pCM⁻ are so well separated in DMF. Because ethylene glycol and DMF have almost the same polarity ($\epsilon \sim 37$), the massive blue shift of the lower absorption band in ethylene glycol can be attributed to the formation of strong solute–solvent hydrogen bonds, the energy of which is weakened upon excitation. The magnitude of this weakening is given by the 3300 cm⁻¹ shift, which is about 10 kcal·mol⁻¹. Conversely, Figure 2 shows that the maximum of the fluorescence spectrum of pCM⁻ and pCT⁻ is not sensitive to the hydrogen-bond donating character of the solvent; it is located almost at the same wavelength in both DMF and ethylene glycol.

This is a remarkable demonstration that, after the Franck–Condon excitation, not only are the hydrogen bonds weakened but also they are in such a way reorganized that, upon radiative return to the ground state, their overall energy is essentially not changed. An alteration of the hydrogen-bond network upon excitation can be expected when the electronic transition involves a significant modification of the electron density on the hydrogen-bond donor–acceptor groups of the solute.⁶⁰ Ab initio and DFT calculations performed on the isolated chromophore (the thioester derivative) indeed predicted an electron shift from the negatively charged phenolate oxygen toward the carbonyl oxygen, upon excitation in the lowest transition.^{49–51} It is important to recall that the photoinduced weakening of the pCM⁻ or pCT⁻ hydrogen-bond network is very large (10 kcal·mol⁻¹); it is in fact close to the total energy of two standard OH···O hydrogen bonds. This fact might be interpreted by the full disruption of two hydrogen bonds, possibly involving the phenolate group, upon electronic excitation.

It is interesting to note that, in native PYP, the phenolate oxygen is known to be bound to the hydroxyl groups of the closest amino acids residues, Glu46 and Tyr42, through two hydrogen bonds. In the protein, the shift of the absorption spectrum associated to the interaction of the chromophore with the residues has been estimated to be about 1000 cm⁻¹.^{61,62} This shift, which is 3 times smaller than the one observed for the denatured PYP²⁵ or pCT⁻ in protic solvents, indicates that the hydrogen bond network between the chromophore and the protein is much less sensitive to the electronic excitation. UV pump–mid-IR probe spectroscopy gave indeed evidence that the hydrogen-bond network involving this negatively charged oxygen is not modified upon electronic excitation.²⁴ One may think that it might be due to the presence of the positively charged Arg52 hampering the electronic redistribution in the chromophore upon excitation.

Solvatochromism. We studied the deprotonated form of the three *trans-p*-hydroxycinnamic acid derivatives in water, in a series of alcohols given in Table 1 and in DMF. Because we have seen that pCM⁻ and pCT⁻ are involved in strong solute–solvent hydrogen bonds in protic solvents, we performed a Kamlet and Taft⁶³ multilinear regression of both the absorption and emission maxima: $\tilde{\nu} = \tilde{\nu}_0 + p \times \pi^* + a \times \alpha$, where π^* and α are respectively the polarity and the hydrogen-bond donor character of the solvent and $\tilde{\nu}_0$ is the wavenumber of the transition in vacuo. The parameters of the fits and the regression coefficients R are reported in Table 2. The solvent parameters used for the fits were taken from ref 64 and are given in Table 1. The calculated absorption and emission maxima versus the observed maxima are represented in Figure 3. For the absorption maximum of pCM⁻ and pCT⁻, R is respectively 0.97 and 0.94. One can see that the main contribution to the absorption

TABLE 1: Solvent Parameters and Steady-State Absorption and Emission Maxima of pCM⁻ and pCT⁻^a

solvent	π^*	α	pCM ⁻		pCT ⁻	
			ν_{abs} (cm ⁻¹)	ν_{em} (cm ⁻¹)	ν_{abs} (cm ⁻¹)	ν_{em} (cm ⁻¹)
water	1.09	1.17	28 902	21 882	25 316	19 945
ethylene glycol	0.92	0.9	28 329	22 222	25 000	20 221
DMF	0.88	0	25 253	22 321	21 413	19 919
methanol	0.6	0.98	28 653	22 472	25 147	20 627
ethanol	0.54	0.86	28 090	22 624	24 414	20 627
1-propanol	0.52	0.84	28 090	22 779	n.m.	n.m.
1-butanol	0.47	0.84	28 090	22 779	24 038	n.m.
1-octanol	0.40	0.77	28 249	23 095	n.m.	n.m.
1-decanol	0.45	0.7	28 329	23 202	24 919	20 867

^a π^* and α are respectively the polarity and the hydrogen-bond donor character of the solvent taken from ref 64. ν_{abs} and ν_{em} are the wavenumbers corresponding to the maxima of the steady-state absorption and emission spectra (n.m. = not measured).

TABLE 2: Parameters of Kamlet and Taft⁶³ Multilinear Regression of the Steady-State Absorption and Emission Maxima of pCM⁻ and pCT⁻^a

compound		ν_0 (cm ⁻¹)	p (cm ⁻¹)	a (cm ⁻¹)	R
pCM ⁻	absorption	25 987	-746	3184	0.97
	emission	23 785	-1599	-184	0.95
pCT ⁻	absorption	22 033	-541	3430	0.94
	emission	21 266	-1505	294	0.99

^a Steady-state absorption and emission maxima were fitted to the multiparametric equation: $\tilde{\nu} = \tilde{\nu}_0 + p \times \pi^* + a \times \alpha$, where π^* and α are respectively the polarity and the hydrogen-bond donor character of the solvent (see Table 1) and $\tilde{\nu}_0$ is the wavenumber of the transition in vacuo. R is the regression coefficient obtained.

solvatochromism is a blue shift proportional to α ($a_{\text{pCM}} = 3184$ cm⁻¹ and $a_{\text{pCT}} = 3430$ cm⁻¹). π^* is found to induce a much smaller red shift ($p_{\text{pCM}} = -746$ cm⁻¹ and $p_{\text{pCT}} = -541$ cm⁻¹). The multilinear fit of the emission spectrum shift confirms the weak impact of the solvent hydrogen-bond donating character on the spectra (a is small). The emission solvatochromism of the three *trans-p*-coumaric acid derivatives is mostly a red shift proportional to the polarity of the solvent. One may relate this effect to the report of a 25 D photoinduced change of dipole moment for thiomethyl *trans-p*-coumarate (measured by Stark spectroscopy at 77 K) in a glycerol–buffer solution.⁴³ It was attributed to a shift of the negative charge from the phenolate oxygen toward the double bond.⁴³ Calculations on the isolated chromophore led to a lower but still significant value of the differential dipole moment, of the order of 9 D.⁵¹

Finally, the considerable red shift (about 50 nm) of the absorption spectra of pCT⁻ with respect to those of pCA²⁻ in alcohols and of pCM⁻ in alcohols and in DMF can be explained by the presence of the thioester group, which has a larger electronic affinity than the carboxylic group or the amide group. The strong influence of the carbonyl tail substituent on the lowest electronic transitions of PYP chromophore analogues appears also in several computational works.^{49,55,62} Substitution of an oxygen atom by a sulfur atom is found to increase the energy of the HOMO orbital and to lower the LUMO orbital energy.⁶²

3.2. Transient Spectroscopy of pCA²⁻ and pCM⁻ in Alcohols. The transient spectra of both compounds in basic alcoholic solutions are qualitatively similar to those recorded previously in water.^{27,29,39,45} Figures 4 and 5 show (a) the differential absorbance spectra of pCA²⁻ and pCM⁻ in ethylene glycol after excitation at 355 nm and (b) the kinetics at two characteristic wavelengths. A positive excited-state absorption

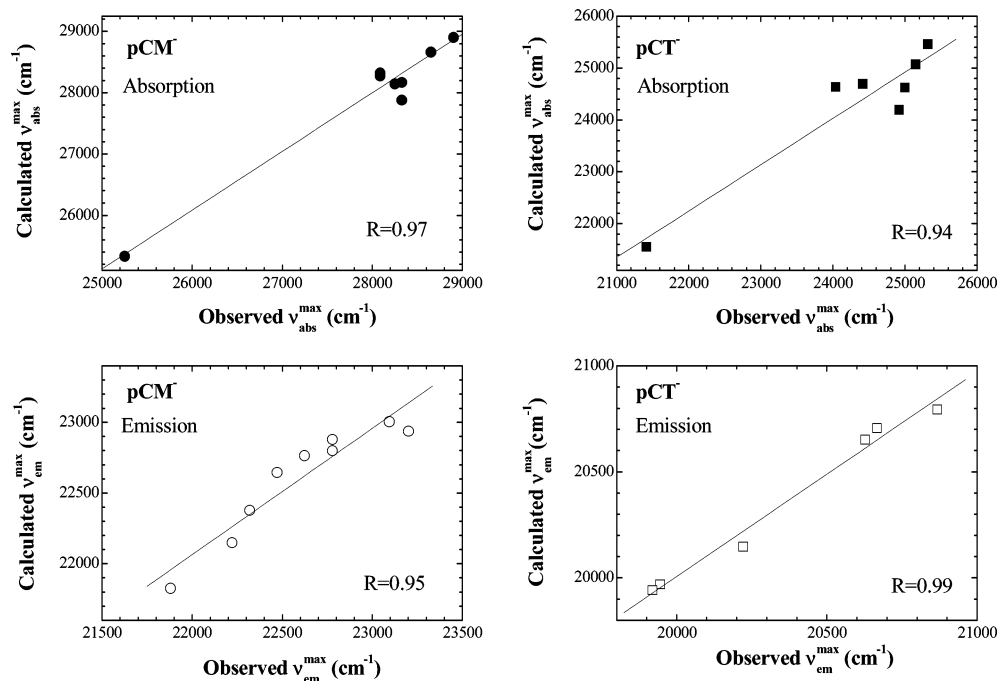


Figure 3. Calculated maxima of the absorption and emission spectra of pCM^- and pCT^- obtained by Kamlet and Taft regression analysis (see Table 2) plotted versus the observed maxima reported in Table 1 in various solvents.

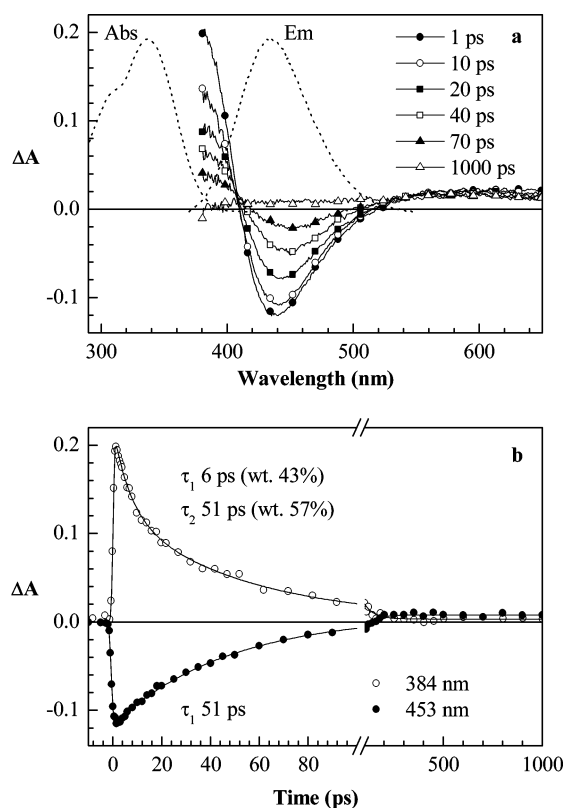


Figure 4. (a) Differential absorbance spectra of pCA^{2-} in ethylene glycol containing 0.05 M KOH recorded after excitation at 355 nm with 0.5 ps laser pulses. The steady-state absorption and fluorescence spectra are shown in dotted lines. (b) Kinetics extracted from the differential spectra at 384 and 453 nm. Data were fitted to a sum of exponentials convoluted with a 1.6 ps (fwhm) Gaussian function representing the experimental response function.

band below 400 nm and a negative stimulated-emission band peaking in the spectral region of the steady-state fluorescence are observed. A weak and broad positive band is also seen above 520 nm. This band is formed instantaneously upon excitation

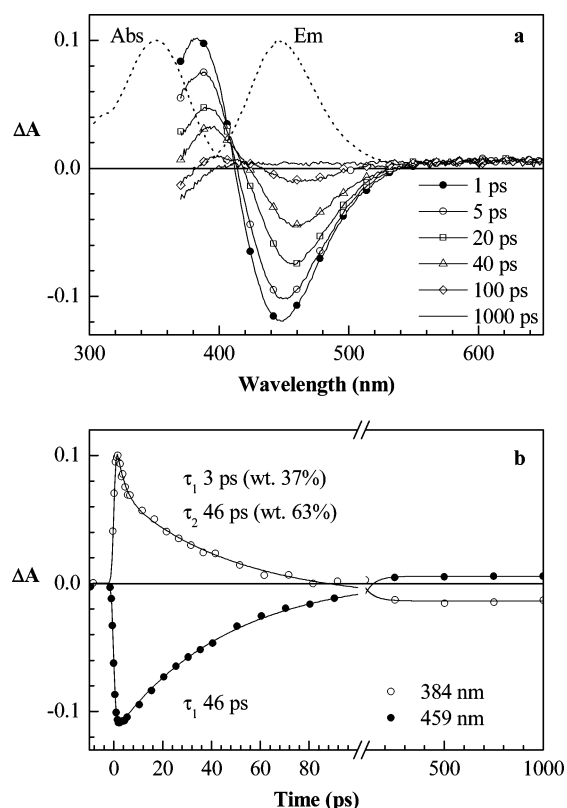


Figure 5. (a) Differential absorbance spectra of pCM^- in ethylene glycol containing 0.05 M KOH recorded after excitation at 355 nm with 0.5 ps laser pulses. The steady-state absorption and fluorescence spectra are shown in dotted lines. (b) Kinetics extracted from the differential spectra at 384 and 459 nm. Data were fitted to a sum of exponentials convoluted with a 1.7 ps (fwhm) Gaussian function representing the experimental response function.

and remains unchanged for all pump–probe delays. By comparison with our previous experiments carried out in water, it is attributed to the absorption of solvated electrons formed by two-photon ionization of the phenolate group.^{27,29,39,45} This

nonlinear process is independent of the one-photon process contributing to the differential spectra in the 340–550 nm spectral region. In a basic aqueous solution, the associated radical (pCA^{\bullet}) absorption band is known to be located around 330 nm in the spectral region of the ground-state absorption, out of our probing range.⁶⁵ One may suppose that the radical absorbs in the same wavelength range in the solvents examined here. On the other hand, a persistent bleaching in the transient spectra of pCM^- is observed once the excited state has completely relaxed (see Figure 5a), seemingly indicating that the initial excited population did not totally return to the initial ground state and that some long-lived photoproduct has been formed. From the ground-state absorption coefficient of pCM^- in ethylene glycol ($15\,200\text{ M}^{-1}\cdot\text{cm}^{-1}$ at 380 nm), one can estimate at $8 \times 10^{-6}\text{ M}$ the concentration of this long-lived species, at 1 ns. In fact, using the absorption coefficient of the solvated electron ($9000\text{ M}^{-1}\cdot\text{cm}^{-1}$ at 600 nm⁶⁶), one can calculate that the concentration of the initially formed radical cation is very close to this value: $7 \times 10^{-6}\text{ M}$. We conclude then that most of the persistent bleaching at 1 ns arises from the partial biphotonic ionization of the molecules and not from a photochemical process following one-photon excitation.

In Figure 4a and Figure 5a, one can also observe a dynamical red shift of the stimulated-emission bands of pCA^{2-} and pCM^- , in a few tens of picoseconds. As expected from the positive solvatochromism of the steady-state fluorescence, this shift is attributed to the solvation dynamics induced by the intramolecular charge translocation upon excitation. In our previous experiments in water,^{27,29,39,40,45} we did not mention such a shift because it is in fact found to occur in about 1 ps, during the rise of the signal. The dynamical Stokes shift in ethylene glycol could be fitted to a single 15 ps exponential, in agreement with the mean solvation time.⁶⁷ In the other alcohols we studied, when the excited-state lifetime is comparable to or shorter than the mean solvation time, the stimulated-emission band decays before the entire solvation process ends. As a consequence, the decays of the stimulated emission are found to be multiexponential and wavelength-dependent. The kinetics in the spectral region close to the maximum of the stimulated-emission band are nevertheless found to be monoexponential (see Figures 4b and 5b) with a time constant of 51 ps for pCA^{2-} and of 46 ps for pCM^- , assigned to the intrinsic lifetime of the excited state.

As seen in Figure 5a, the excited-state absorption band of pCM^- in ethylene glycol also exhibits a time-dependent red shift. This shift is mostly due to its overlap with the persistent ground-state bleaching band that becomes dominant after 60 ps. Consequently, the reduced red shift of the excited-state absorption band of pCA^{2-} , as compared to that of pCM^- , is explained by the negligible contribution of the ground-state bleaching band between 370 and 400 nm. The decay of the excited-state absorption band is biexponential with one time component equal to that of the stimulated-emission band decay and one additional short component of 6 ps (43 wt %) for pCA^{2-} and 3 ps (37 wt %) for pCM^- . Such a fast decay component, was recently reported by Vengris et al. for pCA^{2-} in basic aqueous solution in the subpicosecond regime, and tentatively explained by the presence of several closely spaced excited states simultaneously populated by the laser excitation although no excitation wavelength effect was observed.⁴⁷ By using 300 nm as the excitation wavelength, we indeed did not find much difference in the time-resolved spectra, within our experimental error (data not shown here). At present, we cannot draw a clear conclusion about the nature of the multiexponential decays of the excited-state absorption of pCA^{2-} and pCM^- .

TABLE 3: Excited-State Decay Kinetics of pCA^{2-} and pCM^- in Water and Alcohols^a

solvent	stimulated-emission decay (ps)		η (cP, 25 °C)	ϵ (25 °C)	$\langle\tau_s\rangle$ (ps)
	pCA^{2-}	pCM^-			
methanol	11	12	0.54	32.7	5.0
water	10	4	0.89	78.3	<1
ethanol	14	15	1.07	24.6	16
1-propanol	16	n.m.	1.94	20.5	26
1-butanol	17	n.m.	2.54	17.5	63
1-pentanol	18	n.m.	3.62	13.9	103
1-octanol	21	n.m.	7.29	9.9	
1-decanol	20	(21) ^b	10.9	7.2	245
ethylene glycol	51	46	16.1	37.7	15.3

^a Kinetics are extracted at the maximum of the stimulated-emission band and fitted to a monoexponential function (n.m. = not measured). η , ϵ , and $\langle\tau_s\rangle$ are respectively the viscosity, the dielectric constant and the average solvation time of the different solvents used taken from ref 67. ^b Kinetics of pCM^- in decanol are biexponential with lifetimes of 5 ps (37 wt %) and 32 ps (63 wt %); the average lifetime is reported in the table.

The data extracted from the fit of the excited-state absorption and stimulated-emission decays are given in Table 3, for pCA^{2-} and pCM^- in water and in various alcohols, after excitation at 355 nm. The excited-state lifetimes of pCA^{2-} and pCM^- in the different alcohols are comparable, although the decay of the stimulated emission of pCM^- in 1-decanol is biexponential, whereas in water the lifetime of pCM^- is 2.5 times shorter than that of pCA^{2-} . A weak increase of the excited-state lifetime is observed with increasing solvent viscosity.

3.3. Transient Spectroscopy of pCT^- in Alcohols. *Transient Spectra.* The differential absorbance spectra of pCT^- in ethylene glycol excited at 430 nm are plotted in Figure 6a. They exhibit qualitatively the same features as those obtained in a basic aqueous solution.^{27,29,40,45} Upon excitation, three bands rise instantaneously: the excited-state absorption band in the near UV (ca. 360 nm), the ground-state bleaching band around 430 nm and the stimulated-emission band in the spectral region of the steady-state fluorescence spectrum (ca. 490 nm). At delay times shorter than 50 ps, the maximum of the ground-state bleaching band is red shifted with respect to the steady-state absorption spectrum (430 nm instead of 400 nm), due to the strong contribution of the excited-state absorption. For pump–probe delays up to 50 ps, the three initial bands decay whereas around 450 nm, between the ground-state bleaching and the stimulated-emission bands, an absorption band rises and becomes positive. In the meantime, the stimulated emission band exhibits a dynamical red shift due to solvation dynamics whereas the UV transient absorption band undergoes a slight blue shift.

For pump–probe delays larger than 80 ps, after the decay of both the UV transient absorption and stimulated-emission bands, a small persistent bleaching signal is observed, indicating that part of the excited-state population did not return to the ground state. Unlike pCA^{2-} and pCM^- , steady-state photolysis of pCT^- in basic aqueous solution does not evidence the formation of a stable ground-state cis isomer.⁴⁰ On the contrary, radical cation–solvated electron pairs produced by biphotonic ionization of the phenolate group have been observed in the transient absorption spectra of pCT^- and of *trans*-*S*-thiomethyl-*p*-hydroxycinnamate in water.^{29,42} One may thus think that the present persistent bleaching in ethylene glycol is also due to the biphotonic ionization of pCT^- .

As pointed out in our previous papers,^{27,29,45} the difficulties in the interpretation of the transient spectra of pCT^- arise from the contribution of several overlapping bands. When the

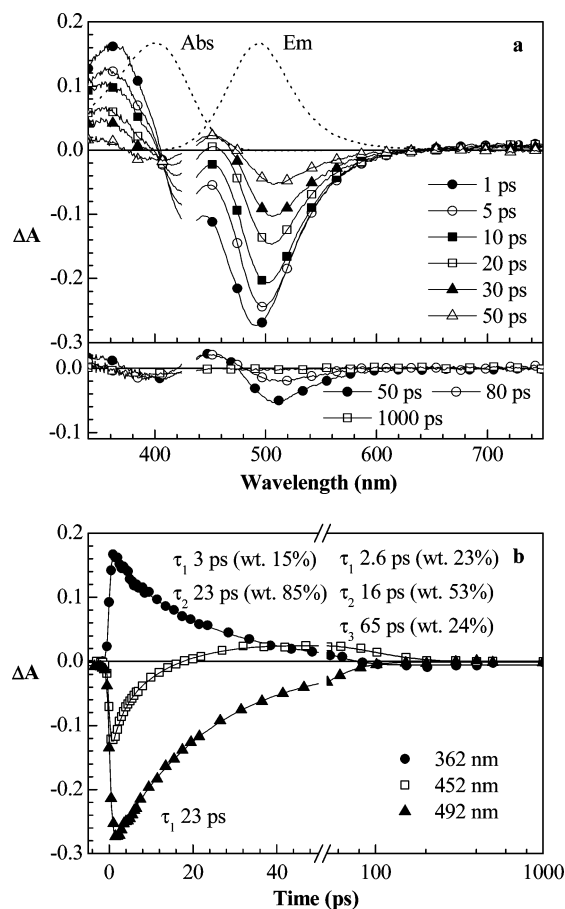


Figure 6. (a) Differential absorbance spectra of pCT⁻ in ethylene glycol containing 1×10^{-3} M KOH recorded after excitation at 430 nm with 0.5 ps laser pulses. The steady-state absorption and fluorescence spectra are shown in dotted lines. (b) Kinetics extracted from the differential spectra at 362, 452, and 492 nm. Data were fitted to a sum of exponentials convoluted with a 1.2 ps (fwhm) Gaussian function representing the experimental response function.

differential absorbance kinetics in the spectral region of the stimulated emission are examined, wavelength-dependent kinetics are observed. The decays on the red side of the stimulated-emission band have been fitted to a biexponential function with a rising component of 3–6 ps, which can be attributed to the dynamical Stokes shift of the band, and a decay component varying from 23 to 34 ps at increasing wavelength. On the red side of the UV excited-state absorption (see Figure 6b) the kinetics are also biexponential with time components of 3 and 23 ps. The fast decay is not observed on the blue side of the band, like in water.^{27,29,45} As illustrated in Figure 6b, the long decay is comparable to the stimulated-emission decay around 500 nm. Finally, between the bleaching and the stimulated-emission bands, around 450 nm, the kinetics are triexponential with components of 2.6, 16, and 65 ps (see Figure 6b). The multiexponential character of this spectral region is likely due to the contribution of several overlapping bands including the red-shifting stimulated emission and the ground-state bleaching, in addition to the intermediate absorption band formed in the course of the excited-state decay. At short time the stimulated emission is expected to dominate the signal at 450 nm ($\Delta A < 0$), so that the two short lifetimes of 2.6 and 16 ps are likely to reflect mostly the dynamical red shift of the stimulated-emission band rather than the formation of the intermediate. On the other hand, the 65 ps component can be attributed unambiguously to the lifetime of the intermediate because, at 450 nm and on this time scale, its absorption is dominant.

TABLE 4: Excited-State Decay Kinetics of pCT⁻ in Water and Alcohols^a

solvent	450 nm		stimulated-emission decay (ps)	η (cP, 25 °C)	ϵ (25 °C)	$\langle \tau_s \rangle$ (ps)
	rise (ps)	decay (ps)				
water	1.0	3.3	2.4	0.89	78.3	<1
methanol	6	9	6	0.54	32.7	5.0
ethanol	8	35	12	1.07	24.6	16
ethylene glycol	2.6, 16	65	23	16.1	37.7	15.3
1-decanol	4, 35	>1 ns	64	10.9	7.2	245

^a Kinetics were extracted at 450 nm and at the maximum of the stimulated-emission band. η , ϵ , and $\langle \tau_s \rangle$ are respectively the viscosity, the dielectric constant and the average solvation time of the different solvents used taken from ref 67.

We previously hypothesized that the complexity of the kinetics across the transient spectra of pCT⁻ in water may result from the excitation of two quasi-degenerate excited states, which could in particular explain the wavelength-dependent and multiexponential decay of the UV excited-state absorption band.^{27,29,45} In a scenario where the upper state would not relax to the lower one, Kasha's rule could be violated and the fluorescence excitation spectrum would be expected to be different from the absorption spectrum. Due to the low fluorescence intensity of the sample and its chemical instability, we could, however, not reach a safe conclusion from the comparison of the absorption and excitation spectra of pCT⁻; the difference lies within the experimental error. On the other hand, we did not observe an excitation-wavelength effect on the time-resolved spectra, within our pump–probe setup experimental error, when tuning the laser excitation wavelength from 430 to 350 nm (data not shown). Multiexponential decays of the UV excited-state absorption band are also observed for pCA²⁻ and pCM⁻ in protic solvents. We might think of a solvatochromic shift of the UV excited-state absorption band although we do not know whether the probed transition is affected by the solvent polarization. One may wonder whether the transient spectra contain the primary dynamics corresponding to the hypothetical breaking of the hydrogen bonds with the solvent upon excitation. Femtosecond visible pump–IR probe of hydrogen-bonded complexes of coumarin 102 and phenol has shown that the hydrogen bond cleavage occurs within 200 fs, followed by the reorganization of the solvent in 800 fs.^{68,69} Concerning the PYP chromophore analogues, no clear conclusion can nevertheless be drawn at the moment.

The kinetics measured in water and various alcohols are given in Table 4. As a general trend, the decay of the bands is slowed down when the viscosity and the mean solvation time increase and when the polarity decreases. The amplitude of this effect, however, depends on the observed band: from methanol to 1-decanol, the stimulated-emission decay is slowed down by a factor of 10 whereas the lifetime of the 450 nm intermediate is increased by a factor of 100. It is difficult to assign the observed effects to one particular property of the solvent. It is nevertheless worth mentioning that the excited-state lifetime of pCT⁻ is more sensitive to the solvent properties than that of pCA²⁻ and pCM⁻. In the Discussion we will further analyze this difference.

It can be noticed from Table 4 that, in most of the solvents, the rise time of the 450 nm intermediate is different from the decay time of the stimulated emission. As pointed out for ethylene glycol, stimulated emission is expected to be dominant at short times in this spectral region, so that solvent-induced time-resolved shift of the stimulated-emission band is expected to contribute to the kinetics. As a matter of fact, the short time components extracted from this region correspond quite well

to the solvation dynamics, except in 1-decanol where the mean solvation time is much slower than the decay of the emission.

Simulations of the Transient Spectra. To check a reaction scheme where the 450 nm transient is formed from the fluorescent excited state, we performed a first simulation of the ΔA spectra with the simple sequential three-state model: $A^* \rightarrow X \rightarrow A$. After excitation, the Franck–Condon excited state (A^*) forms the intermediate-state X corresponding to the 450 nm transient with the rate constant k_1 . X returns to the initial ground-state A with the rate constant k_2 . This model does not provide a good qualitative representation of the ΔA spectra in the bleaching region (between 390 and 440 nm). In the simulation of this spectral region, the signal is found to be constant over the time scale corresponding to the formation time of the 450 nm intermediate, whereas one can see in Figure 6a that it exhibits a fast decay during this time scale. A satisfactory representation of the bleaching region could nevertheless be obtained, in most of the solvents, by introducing a branching reaction from the excited-state A^* , with a ratio of 50% of the excited-state population going back to the ground state and the other 50% forming the 450 nm transient.

In the simulations, the transition cross sections associated with the different bands were approximated by log-normal functions. The stimulated-emission cross section spectrum (shape and intensity) was estimated from the steady-state fluorescence spectrum. The dynamical Stokes shift of the stimulated emission has been simulated according to the solvation dynamics given by Horng et al.⁶⁷ The stimulated-emission spectrum at time zero and the amplitude of the Stokes shift have been estimated from the observed shift and the solvation dynamics given by Horng et al.⁶⁷ The cross section spectrum of the excited-state absorption was determined from the ΔA spectra at time zero after subtraction of the contributions of the ground-state bleaching and of the stimulated emission. The cross section spectrum of the 450 nm transient was extracted from the ΔA spectra measured once the stimulated emission has completely vanished and from which the residual bleaching contribution was subtracted. The decays of the excited-state corresponding to the stimulated-emission decay and the 450 nm transient were represented by an exponential function with time constants reported in Table 4. With the sequential model used here, the rate constants k_1 and k_2 are equal to the inverse of these time constants.

The simulation of the transient spectra of pCT^- in ethylene glycol is represented in Figure 7. Comparison of Figures 6a and 7 shows that our simulation allows a good representation of the transient spectra of pCT^- . Such a result is also obtained in most of the solvents of the Table 4. The agreement found between the simulated and the measured differential spectra is only qualitative because the various parameters of the simulation have not been fitted to the experimental data. We, however, conclude that the excited-state deactivation of pCT^- can reasonably be explained by the formation of the 450-nm transient with a quantum yield of 50% from the fluorescent excited state. It has to be stressed that the solvation dynamics is here implicitly considered to be decoupled from the excited-state deactivation of pCT^- . However, as we will discuss in the next section, we do not exclude that the solvation dynamics could still be a possible reaction coordinate in the excited-state deactivation of pCT^- .

4. Discussion

4.1. Photoisomerization of pCA^{2-} and pCM^- and Reaction Coordinates.

As stated in the Introduction, we previously

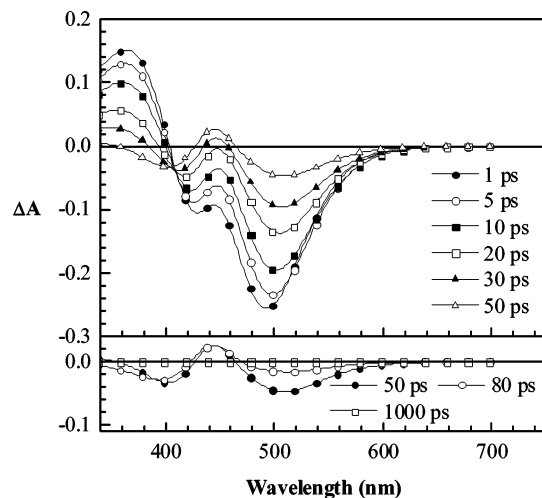


Figure 7. Differential absorbance spectra of pCT^- in ethylene glycol simulated with the sequential three-state model: $A^* \rightarrow X \rightarrow A$. The Franck–Condon excited state, A^* , leads to the formation of the intermediate state, X, corresponding to the 450 nm transient with the rate constant k_1 and a branching ratio of 50%. X returns to the initial ground state with the rate constant k_2 . k_1 and k_2 are fixed to 1/28 and 1/60 ps^{-1} , respectively. The maximum of the stimulated-emission spectrum at time zero is taken at 20 705 cm^{-1} . Amplitude of the shift of the band is fixed at 1173 cm^{-1} and the rate of the shift corresponds to the mean solvation time of 15 ps. Simulated spectra are convoluted with a 1.2 ps (fwhm) Gaussian function representing the experimental response function.

demonstrated that the nonradiative decay of pCA^{2-} and pCM^- in water is correlated to the net trans to cis isomerization reaction that has been shown to take place in those compounds.^{27,29,39,45} By analogy, the concomitant decay of the excited-state absorption and stimulated-emission bands of pCA^{2-} and pCM^- in alcohols, is also attributed to trans to cis isomerization of the ethylenic double bond. More precisely, the trans excited-state is supposed to decay through a small barrier to a nonpopulated intermediate structure (the stilbene-like “perp” configuration⁴⁸) that immediately leads to both the ground-state cis and trans isomers.

Solvent Viscosity Effect. For a variety of systems, the Kramers approach fails to describe the friction a solvent exerts on the crossing rate of a barrier. For *trans*-stilbene, the viscosity dependence of the isomerization rate constant has been shown to be adequately described by the phenomenological power law: $k_{iso} = C\eta^{-a}$, with $0 < a < 1$.^{48,70–76} The parameter a gauges the strength of the solvent damping and C is proportional to the Arrhenius term $\exp(-E_a/kT)$. When k_{iso} is very superior to all other deactivation rates, k_{iso} can be approximated to the reciprocal of the excited-state lifetime (τ_{es}). In Figure 8, the excited-state lifetimes τ_{es} of pCA^{2-} (circles), and pCT^- (triangles) are plotted versus the viscosity η on a log–log scale. Regression analysis for pCA^{2-} is shown in solid line and gives $a = 0.28$. In the case of pCM^- , we did not collect enough experimental data to carry out the same analysis. We can, however, extrapolate from Table 3 that it follows approximately the same power law as pCA^{2-} , except in water.

The a value of 0.28 we found for pCA^{2-} is low compared to stilbenes in alcohols. For reference, a was found to be 0.6 for *trans*-stilbene,⁷⁷ 0.61 for 4,4'-dihydroxystilbene⁷⁶ and 0.72 for 4,4'-dimethoxystilbene.⁷³ Such a nonlinear viscosity dependence has been partly explained by the inadequacy of Kramer's theory to correctly describe friction and Grote and Hynes' theory⁷⁸ was found to be more appropriate to account for the time-dependent friction experienced by the solute.⁷⁰

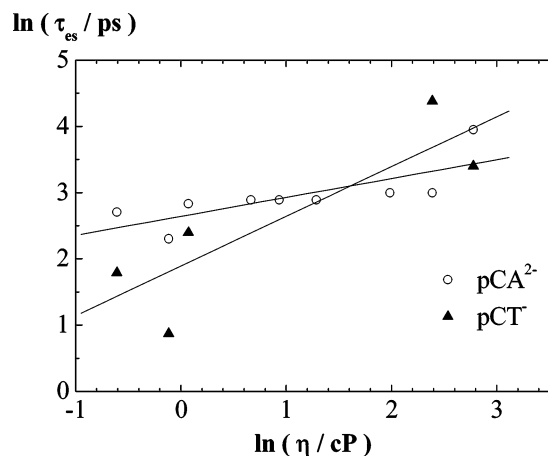


Figure 8. Excited-state lifetime τ_{es} of pCA^{2-} (circles) and pCT^{-} (triangles) represented as a function of the solvent viscosity η . Regression analysis is shown as a solid line and leads to the expression $1/\tau_{es} = C(\eta/cP)^a$ with $a = 0.28$ and 0.75 respectively for pCA^{2-} and pCT^{-} .

On the other hand, the marked deviation to the linear viscosity dependence of *trans*-stilbene and some of its derivatives has also been attributed to the existence of several reaction coordinates. The reaction has been reported to involve two concerted motions: the torsion around the ethylenic bond and the adjacent single-bond rotation.^{70,74,79} In this multidimensional picture of the reaction, the viscosity effect is expected to be weaker than expected for a mechanism involving only the torsion around the double-bond.^{70,79,80} Stiff-stilbene (1,1'-diindanylidene), where torsion around the single-bonds is hindered, isomerizes along a reaction coordinate that is probably closer to this "ideal" one-dimensional case. In this case, the viscosity dependence of the formation rate of the "perp" state is found to be quasi linear.⁸¹ Within this context, one might thus think that the photoisomerization of pCA^{2-} and pCM^{-} involves the concerted torsion of two bonds rather than the single rotation of the ethylenic bond.

Solvent Polarity Effect. In addition to the solvent viscosity, solvent polarity can affect the isomerization rate of pCA^{2-} and pCM^{-} . In the studied alcohol series, when the viscosity η increases, the dielectric constant ϵ decreases, as can be seen in Table 3. The decrease of the photoisomerization rate in solvents of lower dielectric constant may indicate an increase of the activation energy, which would arise from the "perp" state being more polar than the initial fluorescent state. In addition to this static effect, it is worth noting that the isomerization rate of pCA^{2-} and pCM^{-} in linear alcohols (except methanol; see Table 3) is faster than the average solvation dynamics, indicating that the reaction occurs in a nonequilibrated solvent configuration. This, however, does not allow us to rule out the possible participation of solvation in the reaction^{76,82–84} because it can be argued that only the short times of the solvation dynamics are involved in the reaction.

4.2. Photoisomerization of pCT^{-} and Reaction Coordinates. The transient spectroscopy of pCT^{-} in aqueous solution revealed that its excited-state relaxation mechanism is quite different from those of pCA^{2-} and pCM^{-} . It proceeds through a more complex pathway, involving the formation, on the picosecond time scale, of an intermediate absorbing around 450 nm between the bleaching and the stimulated-emission bands, in all solvents studied here.^{27,29,40,45} Formation of this intermediate was also reported for *trans*-*p*-hydroxythiomethyl cinnamate in basic aqueous solution.^{41,42,44,47}

Excited-State Decay and Solvent Effects. Although the data for pCT^{-} are scarce and scattered, it is interesting to note that the decay of its stimulated-emission band appears to be much more sensitive to the solvent than those of pCA^{2-} and pCM^{-} . A very coarse analysis of the solvent viscosity effect is shown in Figure 8. The rough fit leads to $1/\tau_{es} \approx C\eta^{-a}$, with a being equal to 0.75, that is, about 3 times larger than the value found for pCA^{2-} . In addition, we observe that the sensitivity of the excited-state dynamics of pCT^{-} to the solvent polarity and solvation dynamics is larger than for pCA^{2-} and pCM^{-} . In low viscosity solvents, the excited-state lifetime of pCA^{2-} does not change much when the dielectric constant increases whereas that of pCT^{-} keeps decreasing. The most natural explanation for these differences is that the excited-state deactivation involves either a different reaction coordinate or a different reaction profile along the same coordinate.

The larger electronic affinity of the thioester substituent of pCT^{-} , as compared to pCA^{2-} and pCM^{-} , can induce a larger further charge translocation after excitation. For pCA^{2-} the transfer of a full charge cannot reach the carboxylic group due to the presence of the negatively charged oxygen atom whereas for pCT^{-} the electron can be transferred to the oxygen atom of the carbonyl group. In this simple representation, it is conceivable that the reaction coordinates in the excited state could be different in these two compounds. Like for *trans*-stilbene, the concerted motions of the ethylenic bond and one adjacent single bond would still be possible in the excited state for pCA^{2-} . For pCT^{-} only the torsional motion of the ethylenic bond would be facilitated because the adjacent single bonds would acquire a double bond character upon charge translocation. These differences in the reaction coordinates could explain the larger impact of the solvent viscosity on the excited-state decay of pCT^{-} . It is worth noting that the single torsion of the ethylenic bond (one bond flip) has recently been proposed for the photoisomerization mechanism of charged conjugated systems, such as protonated Schiff bases, whereas isomerization of weakly polar olefins is attributed to the concerted motion of the ethylenic bond with an adjacent single bond.⁸⁵

Relaxation Pathway. Let us here examine three different hypothesis aimed at elucidating the relaxation pathway in pCT^{-} and the nature of the 450 nm intermediate state. At this point of the discussion, it should be reminded that, contrary to pCA^{2-} and pCM^{-} continuous irradiation of pCT^{-} in aqueous solution did not lead to the observation of a *cis* isomer.^{27,29,40,45} The fluorescence quantum yield of pCT^{-} remains, however, comparable to those of pCA^{2-} and pCM^{-} , indicating that an efficient nonradiative process also takes place in the thioester derivative.

(1) Assuming that the photoisomerization reaction occurs in pCT^{-} , it is tempting to attribute the 450 nm intermediate to an unstable ground-state *cis* isomer. However, calculations do not predict the existence of such an unstable ground-state *cis* isomer. Like for pCA^{2-} , the *cis* to *trans* isomerization barrier of the isolated pCT^{-} and thiomethyl coumarate is found to be quite large, about 25 kcal·mol⁻¹.^{49,53} This hypothesis must consequently be rejected.

(2) Alternatively, the higher sensitivity of the excited-state lifetime of pCT^{-} to the solvent polarity and the larger electronic affinity of the thioester group with respect to the carboxylic group of pCA^{2-} and the amide group of pCM^{-} can suggest the formation of a charge-transfer state in competition with isomerization. The merocyanine dye DCM⁸⁶ and some "push-pull" polyenes^{87,88} provide examples of a photoinduced charge transfer in competition with photoisomerization. Considering the concept of TICT-state formation, i.e., an excited-state charge-transfer

reaction concerted with the single-bond rotation of the electron-donating group,⁸⁹ we proposed²⁹ that such a mechanism might compete with photoisomerization for pCT^- , whereas photoisomerization would prevail for pCA^{2-} and pCM^- . Such a TICT-state formation was indeed proposed for “push–pull” stilbenes.^{90,91} For the present analogues, one might think that torsion of the phenolate group could be the proper coordinate leading to a TICT-like state. In a recent report on ester analogues of PYP chromophore,⁹² the torsion of the phenolate group was indeed proposed to be one possible coordinate for the nonradiative excited-state decay. On the other hand, QM/MM simulations carried out on the isolated deprotonated PYP chromophore showed that the evolution on S_1 after photoexcitation involves the torsion of the phenolate moiety rather than the ethylenic bond torsion. On the time scale of the simulation, the population remains trapped in a local S_1 minimum associated with a 90° twisted phenolate moiety.⁵⁴ The excited-state deactivation leads back to the original conformation without a net change of configuration. However, one can object to a process involving such a coordinate that, in agreement with an elementary view considering that the lower electronic transition essentially shifts the charge from the phenolate moiety to the carbonyl moiety, other ab initio calculations predicted a reversal of the single/double bond pattern of the molecule upon excitation.⁵⁰ The single bond linking the phenolate group to the rest of the molecule acquires a double bond character and the ethylenic bond acquires a single bond character. According to this picture, the rotation of the phenolate group should no longer be possible whereas isomerization around the ethylenic bond should be made easier.

(3) Finally, one can consider the photoisomerization coordinate, by rotation around the ethylenic bond alone and refer to a well-known model for the isomerization of polar olefins in polar solvents. It has been proposed that the excited state of these molecules at the “perp” configuration is zwitterionic. In polar solvents, the energy of this “perp” zwitterionic state is strongly lowered and becomes lower than that of the diabatic state representing the ground state in nonpolar solvents. The avoided crossing between the two potential energy surfaces leads to a new minimum at the “perp” configuration in the ground state.⁹³ A somewhat similar situation can be devised for pCT^- . One could think that increasing the electron affinity of the carbonyl substituent from pCA^{2-} , to pCM^- and pCT^- is able to induce a strong lowering of the “perp” excited state with respect to the ground state. For pCT^- , a local minimum of the ground state could be obtained in the “perp” configuration (see Figure 9). Due to the destabilization of the cis isomer in the ground state, the barrier from the “perp” minimum to the cis would be higher than that to the initial trans configuration, resulting in no net trans-to-cis isomerization. This scenario would be totally compatible with the three-state model we used for our simulations of the ΔA spectra, including the loss of 50% of the initial excited population accompanying the formation of the transient state.

5. Conclusion

Solvent effects on the excited-state decay of three analogues of the chromophore of PYP, where the substituent adjacent to the carbonyl end group is changed from O^- (pCA^{2-}) to NH_2 (pCM^-) and to SC_6H_5 (pCT^-), have been examined by steady-state and ultrafast time-resolved spectroscopy. The major solvent effect on the steady-state absorption spectrum is due to the formation of strong hydrogen bonds in protic solvents whereas the fluorescence solvatochromic shift is mainly correlated to

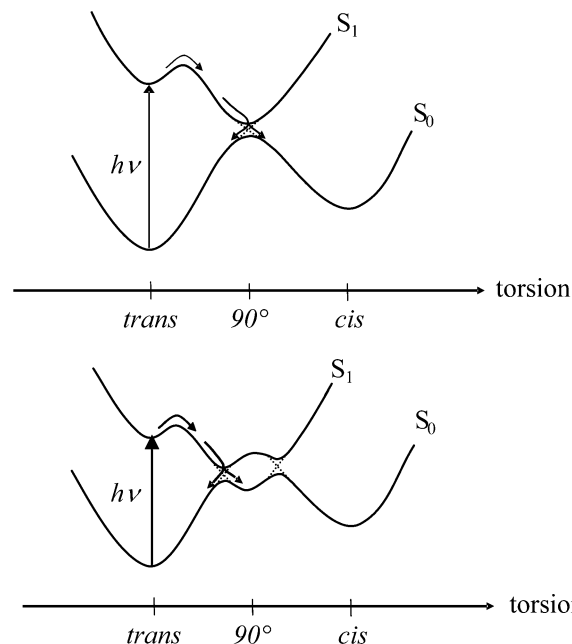


Figure 9. Potential energy curves proposed for the excited-state deactivation of pCA^{2-} (up) pCT^- (down).

the solvent polarity. Our data are consistent with the complete disruption of two hydrogen bonds in the excited state. Fluorescence anisotropy measurements evidence that a second electronic transition with a different polarization, possibly the $n \rightarrow \pi^*$ transition localized on the carbonyl group, contributes to the blue side of the absorption spectra of pCA^{2-} and pCM^- . However, contrary to previous statements,^{27,29,40} the presence of a second transition lying under the main absorption band is not confirmed for pCT^- .

The difference that we previously reported between the differential absorbance spectra of pCT^- and those of pCA^{2-} and pCM^- in aqueous solutions is also found in several alcohols. In addition, the excited-state decay of these compounds is found to be sensitive to the solvent properties. These differences are attributed to the existence of two different relaxation pathways in relation with the electron donor–acceptor character of the chromophore substituents. Upon excitation, analogues with a weaker electron acceptor group such as pCA^{2-} and pCM^- lead to the formation of a cis isomer without any detectable intermediate. On the contrary, excited-state deactivation of analogues containing a stronger electron acceptor group such as pCT^- involve the formation of a transient state absorbing between the bleaching and stimulated-emission band. Additionally, the formation of a stable cis isomer is not observed. Due to the weak sensitivity of the excited-state decay of pCA^{2-} and pCM^- to the solvent viscosity, the photoisomerization mechanism of pCA^{2-} and pCM^- is thought to be comparable to that of *trans*-stilbene, with the concerted rotation of the ethylenic bond and one adjacent single bond. The higher sensitivity of the excited-state deactivation of pCT^- to solvent viscosity and polarity, as compared to pCA^{2-} and pCM^- , is considered to reveal a different reaction coordinate. The excited-state deactivation of pCT^- is viewed as a photoisomerization mechanism involving mainly the torsional motion of the ethylenic bond. The formation of the transient state of pCT^- is tentatively attributed to the existence of a local minimum in the ground state, corresponding to a “perp” conformation having a charge-transfer character, from which the population returns solely to the initial trans conformation.

Acknowledgment. We acknowledge financial support from a CNRS-DFG bilateral project within the framework of the CERC3 initiative. We also thank Prof. Ludovic Jullien and Prof. Jean-Bernard Baudin for providing the amide and the phenylthioester analogues, which have been synthesized on purpose.

References and Notes

- Häder, D.-P.; Lebert, M. *Photomovement*; Elsevier: Amsterdam, 2001.
- Meyer, T. E. *Biochim. Biophys. Acta* **1985**, *806*, 175.
- Sprenger, W. W.; Hoff, W. D.; Armitage, J. P.; Hellingwerf, K. J. *J. Bacteriol.* **1993**, *175*, 3096.
- Baca, M.; Borgstahl, G. E. O.; Boissinot, M.; Burke, P. M.; Williams, D. R.; Slater, K. A.; Getzoff, E. D. *Biochemistry* **1994**, *33*, 14369.
- Hoff, W. D.; Düx, P.; Hard, K.; Devreese, B.; Nugteren-Roodzant, I. M.; Crielgaard, W.; Boelens, R.; Kaptein, R.; van Beeumen, J. J.; Hellingwerf, K. J. *Biochemistry* **1994**, *33*, 13959.
- Borgstahl, G. E. O.; Williams, D. R.; Getzoff, E. D. *Biochemistry* **1995**, *34*, 6278.
- Düx, P.; Rubinstenn, G.; Vuister, G. W.; Boelens, R.; Mulder, F. A. A.; Hard, K.; Hoff, W. D.; Kroon, A. R.; Crielgaard, W.; Hellingwerf, K. J.; Kaptein, R. *Biochemistry* **1998**, *37*, 12689.
- Kim, M.; Mathies, R. A.; Hoff, W. D.; Hellingwerf, K. J. *Biochemistry* **1995**, *34*, 12669.
- Brudler, R.; Rammelsberg, R.; Woo, T. T.; Getzoff, E. D.; Gerwert, K. *Nat. Struct. Biol.* **2001**, *8*, 265.
- Genick, U. K.; Borgstahl, G. E. O.; Ng, K.; Ren, Z.; Pradervand, C.; Burke, P. M.; Srajer, V.; Teng, T.-Y.; Schildkamp, W.; McRee, D. E.; Moffat, K.; Getzoff, E. D. *Science* **1997**, *275*, 1471.
- Unno, M.; Kumauchi, M.; Sasaki, J.; Tokunaga, F.; Yamauchi, S. *J. Am. Chem. Soc.* **2000**, *122*, 4233.
- Unno, M.; Kumauchi, M.; Sasaki, J.; Tokunaga, F.; Yamauchi, S. *Biochemistry* **2002**, *41*, 5668.
- Perman, B.; Srajer, V.; Ren, Z.; Teng, T.-Y.; Pradervand, C.; Ursby, T.; Bourgeois, D.; Schotte, F.; Wulff, M.; Kort, R.; Hellingwerf, K. J.; Moffat, K. *Science* **1998**, *279*, 1946.
- Hoff, W. D.; van Stokkum, I. H. M.; van Ramesdonk, H. J.; van Brederode, M. E.; Brouwer, A. M.; Fitch, J. C.; Meyer, T. E.; van Grondelle, R.; Hellingwerf, K. J. *Biophys. J.* **1994**, *67*, 1691.
- Chosrowjan, H.; Mataga, N.; Nakashima, N.; Imamoto, Y.; Tokunaga, F. *Chem. Phys. Lett.* **1997**, *270*, 267.
- Baltuska, A.; van Stokkum, I. H. M.; Kroon, A. R.; Monshouwer, R.; Hellingwerf, K. J.; van Grondelle, R. *Chem. Phys. Lett.* **1997**, *270*, 263.
- Ujj, L.; Devanathan, S.; Meyer, T. E.; Cusanovich, M. A.; Tollin, G.; Atkinson, G. H. *Biophys. J.* **1998**, *75*, 406.
- Changenet-Barret, P.; Zhang, H.; van der Meer, M. J.; Hellingwerf, K. J.; Glasbeek, M. *Chem. Phys. Lett.* **1998**, *282*, 276.
- Devanathan, S.; Pacheco, A.; Ujj, L.; Cusanovich, M. A.; Tollin, G.; Lin, S.; Woodbury, N. *Biophys. J.* **1999**, *77*, 1017.
- Mataga, N.; Chosrowjan, H.; Shibata, Y.; Imamoto, Y.; Tokunaga, F. *J. Phys. Chem. B* **2000**, *104*, 5191.
- Imamoto, Y.; Kataoka, M.; Tokunaga, F.; Asahi, T.; Masuhara, H. *Biochemistry* **2001**, *40*, 6047.
- Hanada, H.; Kanematsu, Y.; Kinoshita, S.; Kumauchi, M.; Sasaki, J.; Tokunaga, F. *J. Lumin.* **2001**, *94–95*, 593.
- Gensch, T.; Gradinaru, C. C.; van Stokkum, I. H. M.; Hendricks, J.; Hellingwerf, K. J.; van Grondelle, R. *Chem. Phys. Lett.* **2002**, *356*, 347.
- Groot, M. L.; van Wilderen, L. J. G. W.; Larsen, D. S.; van der Horst, M. A.; van Stokkum, I. H. M.; Hellingwerf, K. J.; van Grondelle, R. *Biochemistry* **2003**, *42*, 10054.
- Changenet-Barret, P.; Espagne, A.; Plaza, P.; Martin, M. M.; Hellingwerf, K. J. *Femtochemistry and Femtobiology, Ultrafast events in molecular science*; Martin, M. M., Hynes, J. T., Eds.; Elsevier: Amsterdam, 2004; p 417.
- Larsen, D. S.; van Stokkum, I. H. M.; Vengris, M.; van der Horst, M. A.; de Weerd, F. L.; Hellingwerf, K. J.; van Grondelle, R. *Biophys. J.* **2004**, *87*, 1858.
- Changenet-Barret, P.; Espagne, A.; Charier, S.; Baudin, J.-B.; Jullien, L.; Plaza, P.; Hellingwerf, K. J.; Martin, M. M. *Photochem. Photobiol. Sci.* **2004**, *3*, 823.
- Mataga, N.; Chosrowjan, H.; Taniguchi, S. *J. Photochem. Photobiol. C: Photochem. Rev.* **2004**, *5*, 155.
- Changenet-Barret, P.; Espagne, A.; Plaza, P.; Hellingwerf, K. J.; Martin, M. M. *New J. Chem.* **2005**, *29*, 527.
- Kort, R.; Vonk, H.; Xu, X.; Hoff, W. D.; Crielgaard, W.; Hellingwerf, K. J. *FEBS Lett.* **1996**, *382*, 73.
- Genick, U. K.; Soltis, S. M.; Kuhn, P.; Canestrelli, I. L.; Getzoff, E. D. *Nature* **1998**, *392*, 206.
- Ren, Z.; Perman, B.; Srajer, V.; Teng, T.-Y.; Pradervand, C.; Bourgeois, D.; Schotte, F.; Ursby, T.; Kort, R.; Wulff, M.; Moffat, K. *Biochemistry* **2001**, *2001*, 13788.
- Mataga, N.; Chosrowjan, H.; Shibata, Y.; Imamoto, Y.; Kataoka, M.; Tokunaga, F. *Chem. Phys. Lett.* **2002**, *352*, 220.
- Mataga, N.; Chosrowjan, H.; Taniguchi, S.; Hamada, N.; Tokunaga, F.; Imamoto, Y.; Kataoka, M. *Phys. Chem. Chem. Phys.* **2003**, *5*, 2454.
- Nakamura, R.; Kanematsu, Y.; Kumauchi, M.; Hamada, N.; Tokunaga, F. *J. Lumin.* **2003**, *102–103*, 21.
- Premvardhan, L. L.; van der Horst, M. A.; Hellingwerf, K. J.; van Grondelle, R. *Biophys. J.* **2003**, *84*, 3226.
- Chosrowjan, H.; Taniguchi, S.; Mataga, N.; Unno, M.; Yamauchi, S.; Hamada, N.; Kumauchi, M.; Tokunaga, F. *J. Phys. Chem. B* **2004**, *108*, 2686.
- Kort, R.; Hellingwerf, K. J.; Ravelli, R. B. G. *J. Biol. Chem.* **2004**, *279*, 26417.
- Changenet-Barret, P.; Plaza, P.; Martin, M. M. *Chem. Phys. Lett.* **2001**, *336*, 439.
- Changenet-Barret, P.; Espagne, A.; Katsonis, N.; Charier, S.; Baudin, J.-B.; Jullien, L.; Plaza, P.; Martin, M. M. *Chem. Phys. Lett.* **2002**, *365*, 285.
- Larsen, D. S.; Vengris, M.; van Stokkum, I. H. M.; van der Horst, M. A.; Cordfunke, R. A.; Hellingwerf, K. J.; van Grondelle, R. *Chem. Phys. Lett.* **2003**, *369*, 563.
- Larsen, D. S.; Vengris, M.; van Stokkum, I. H. M.; van der Horst, M. A.; de Weerd, F. L.; Hellingwerf, K. J.; van Grondelle, R. *Biophys. J.* **2004**, *86*, 2538.
- Premvardhan, L. L.; Buda, F.; van der Horst, M. A.; Lührs, D. C.; Hellingwerf, K. J.; van Grondelle, R. *J. Phys. Chem. B* **2004**, *108*, 5138.
- Vengris, M.; van der Horst, M. A.; Zgrablic, G.; van Stokkum, I. H. M.; Haacke, S.; Chergui, M.; Hellingwerf, K. J.; van Grondelle, R.; Larsen, D. S. *Biophys. J.* **2004**, *87*, 1848.
- Espagne, A.; Changenet-Barret, P.; Katsonis, N.; Charier, S.; Baudin, J.-B.; Jullien, L.; Plaza, P.; Martin, M. M. *Femtochemistry and Femtobiology, Ultrafast events in molecular science*; Martin, M. M., Hynes, J. T., Eds.; Elsevier: Amsterdam, 2004; p 431.
- Usman, A.; Mohammed, O. F.; Heyne, K.; Dreyer, J.; Nibbering, E. T. J. *Chem. Phys. Lett.* **2005**, *401*, 157.
- Vengris, M.; Larsen, D. S.; van der Horst, M. A.; Larsen, O. F. A.; Hellingwerf, K. J.; van Grondelle, R. *J. Phys. Chem. B* **2005**, *109*, 4197.
- Waldeck, D. H. *Chem. Rev.* **1991**, *91*, 415.
- Sergi, A.; Grüning, M.; Ferrario, M.; Buda, F. *J. Phys. Chem. B* **2001**, *105*, 4386.
- Molina, V.; Merchan, M. *Proc. Natl. Acad. Sci. U.S.A.* **2001**, *98*, 4299.
- Groenof, G.; Lensink, M. F.; Berendsen, H. J. C.; Snijders, J. G.; Mark, A. E. *Proteins* **2002**, *48*, 202.
- Ko, C.; Levine, B.; Toniolo, A.; Olsen, S.; Werner, H.-J.; Martinez, T. J. *J. Am. Chem. Soc.* **2003**, *125*, 12710.
- Thompson, M. J.; Bashford, D.; Noodleman, L.; Getzoff, E. D. *J. Am. Chem. Soc.* **2003**, *125*, 8186.
- Groenof, G.; Bouxin-Cademartory, M.; Hess, B.; de Visser, S. P.; Berendsen, H. J. C.; Olivucci, M.; Mark, A. E.; Robb, M. A. *J. Am. Chem. Soc.* **2004**, *126*, 4228.
- Gromov, E. V.; Burghardt, I.; Köppel, H.; Cederbaum, L. S. *J. Phys. Chem. A* **2005**, *109*, 4623.
- Liu, R. S. H. *Acc. Chem. Res.* **2001**, *34*, 555.
- Lakowicz, R. *Principles of fluorescence spectroscopy*; Plenum Press: New York, 1983.
- Dai Hung, N.; Plaza, P.; Martin, M. M.; Meyer, Y. H. *Appl. Opt.* **1992**, *31*, 7046.
- Borucki, B.; Otto, H.; Meyer, T. E.; Cusanovich, M. A.; Heyn, M. P. *J. Phys. Chem. B* **2005**, *109*, 629.
- Mataga, N.; Kubota, T. *Molecular Interactions and Electronic Spectra*; Marcel Dekker: New York, 1970.
- Kroon, A. R.; Hoff, W. D.; Fennema, H. P. M.; Koomen, G.-J.; Verhoeven, J. W.; Crielgaard, W.; Hellingwerf, K. J. *J. Biol. Chem.* **1996**, *271*, 31949.
- Yoda, M.; Houjou, H.; Inoue, Y.; Sakurai, M. *J. Phys. Chem. B* **2001**, *105*, 9887.
- Fong, C. W.; Kamlet, M. J.; Taft, R. W. *J. Org. Chem.* **1983**, *48*, 832.
- Marcus, Y. *Chem. Soc. Rev.* **1993**, *22*, 409.
- Foley, S.; Navaratnam, S.; McGarvey, D. J.; Land, E. J.; Truscott, T. G.; Rice-Evans, C. *Free Rad. Biol. Med.* **1999**, *26*, 1202.
- Jou, F.-Y.; Freeman, G. R. *Can. J. Chem.* **1979**, *57*, 591.
- Horng, M. L.; Gardecki, J. A.; Papazyan, A.; Maroncelli, M. *J. Phys. Chem.* **1995**, *99*, 17311.
- Chudoba, C.; Nibbering, E. T. J.; Elsaesser, T. *J. Phys. Chem. A* **1999**, *103*, 5625.
- Nibbering, E. T. J.; Tschirschwitz, F.; Chudoba, C.; Elsaesser, T. *J. Phys. Chem. A* **2000**, *104*, 4236.
- Rothenberger, G.; Negus, D. K.; Hochstrasser, R. M. *J. Chem. Phys.* **1983**, *79*, 5360.
- Courtney, S. H.; Fleming, G. R. *J. Chem. Phys.* **1985**, *83*, 215.
- Troe, J. *J. Phys. Chem.* **1986**, *90*, 357.

- (73) Zeglinski, D. M.; Waldeck, D. H. *J. Phys. Chem.* **1988**, *92*, 692.
(74) Park, N. S.; Waldeck, D. H. *J. Chem. Phys.* **1989**, *91*, 943.
(75) Sivakumar, N.; Hoburg, E. A.; Waldeck, D. H. *J. Chem. Phys.* **1989**, *90*, 2305.
(76) Park, N. S.; Waldeck, D. H. *J. Phys. Chem.* **1990**, *94*, 662.
(77) Sundström, V.; Gillbro, T. *Chem. Phys. Lett.* **1984**, *109*, 538.
(78) Grote, R. F.; Hynes, J. T. *J. Chem. Phys.* **1980**, *73*, 2715.
(79) Lee, M.; Haseltine, J. N.; Smith, A. B., III; Hochstrasser, R. M. *J. Am. Chem. Soc.* **1989**, *111*, 5044.
(80) Schroeder, J.; Schwarzer, D.; Troe, J.; Voss, F. *J. Chem. Phys.* **1990**, *93*, 2393.
(81) Doany, F. E.; Heilweil, E. J.; Moore, R.; Hochstrasser, R. M. *J. Chem. Phys.* **1984**, *80*, 201.
(82) van der Zwan, G.; Hynes, J. T. *Chem. Phys.* **1984**, *90*, 21.
(83) Kim, S. M.; Courtney, S. H.; Fleming, G. R. *Chem. Phys. Lett.* **1989**, *156*, 543.
(84) Mohrschladt, R.; Schroeder, J.; Schwarzer, D.; Troe, J.; Vöhringer, P. *J. Chem. Phys.* **1994**, *101*, 7566.
(85) Sampedro Ruiz, D.; Cembran, A.; Garavelli, M.; Olivucci, M.; Fuss, W. *Photochem. Photobiol.* **2002**, *76*, 622.
(86) Martin, M. M.; Plaza, P.; Meyer, Y. H. *Chem. Phys.* **1995**, *192*, 367.
(87) Plaza, P.; Laage, D.; Martin, M. M.; Alain, V.; Blanchard-Desce, M.; Thompson, W. H.; Hynes, J. T. *J. Phys. Chem. A* **2000**, *104*, 2396.
(88) Laage, D.; Plaza, P.; Blanchard-Desce, M.; Martin, M. M. *Photochem. Photobiol. Sci.* **2002**, *1*, 526.
(89) Grabowski, Z. R.; Rotkiewicz, K.; Rettig, W. *Chem. Rev.* **2003**, *103*, 3899.
(90) Lapouyade, R.; Czeschka, K.; Majenz, W.; Rettig, W.; Gilabert, E.; Rullière, C. *J. Phys. Chem.* **1992**, *96*, 9643.
(91) Rettig, W.; Majenz, W.; Lapouyade, R.; Haucke, G. *J. Photochem. Photobiol. A: Chem.* **1992**, *62*, 415.
(92) El-Gezawy, H.; Rettig, W.; Danel, A.; Jonusauskas, G. *J. Phys. Chem. B* **2005**, *109*, 18699.
(93) Dauben, W. G.; Salem, L.; Turro, N. J. *Acc. Chem. Res.* **1975**, *8*, 41.